

Electronic Supplementary Information

Polyether-based solid electrolytes with a homogeneous polymer network: effect of the salt concentration on the Li-ion coordination structure

Namie Ikeda,^a Asumi Ishikawa,^a and Kenta Fujii^{a}*

Graduate School of Sciences and Technology for Innovation, Yamaguchi University, 1-16-2
Tokiwadai, Ube, Yamaguchi 755-8611, Japan

* To whom correspondence should be addressed. E-mail: k-fujii@yamaguchi-u.ac.jp

Experimental and computational methods.

UV spectra was recorded using UV-vis spectrophotometer (V-730, Jasco) to investigate gelation kinetics. The two polymer solutions (i.e., 10 wt% TetraPEG-MA and TetraPEG-SH in LiTFSA/BN solutions with a fixed Li salt/ O_{PEG} ratio of 1:10, 1:4, or 1:1) were mixed and stirred for 30 s, and then poured into a quartz cell of 0.2 cm thickness. The time dependences of the UV spectra were measured at a time interval of 600 s. The absorbance at 300 nm (A_{300}), which is attributed to the unreacted MA terminals within the TetraPEG-MA, was monitored as a function of reaction time (t). Using the A_{300} , the concentration of unreacted MA was plotted as a function of gelation time (t). A_{300} at the i -th time point, i , is given as $A_{300,i} = \epsilon_{300}l[-\text{MA}]_i$, where ϵ_{300} is the molar absorption coefficient of MA and l is the cell thickness. The concentration of the cross-linking MA-S bond ($[\text{MA-S}]_i$) is described by $[\text{MA-S}]_i = [-\text{MA}]_{\text{ini}} - [-\text{MA}]_i$, where $[-\text{MA}]_{\text{ini}}$ is the initial concentration of MA groups. Thus, the following equation is obtained: $[\text{MA-S}]_i = [-\text{MA}]_{\text{ini}} - A_{300,i}/\epsilon_{300}l$. As established in our previous studies,^{1,2} the PEG-based gelation (i.e., tetra-PEG-MA + tetra-PEG-SH \rightarrow tetra-PEG-MA-S-tetra-PEG) proceeds as a following second-order rate equation:

$$d \frac{[\text{MA-S}]}{dt} \left(= - \frac{d[-\text{MA}]}{dt} \right) = k_{\text{gel}}' [-\text{MA}]_i [-\text{SH}]_{\text{total}, i}$$

where k_{gel}' is an apparent reaction rate constant and $[-\text{SH}]_{\text{total}, i}$ is the total concentration of the unreacted SH groups at the i -th time point. Based on the rate equation, we performed a least-squares fitting analysis by minimizing the error square sum, $U = \Sigma([\text{MA-S}]_{i, \text{exp}} - [\text{MA-S}]_{i, \text{calc}})^2$.

Stretching measurements were performed using mechanical testing apparatus (STB-1225S, A&D Company) at a constant velocity of 30 mm min⁻¹. The dumbbell-shaped TetraPEG electrolytes with Li/ O_{PEG} = 1:10, 1:4, and 1:1 were prepared and the size of a rectangular portion was measured using vernier caliper. The ionic conductivity was measured by AC impedance spectroscopy using a frequency response analyzer (SP-150, Bio-Logic), which is measured in frequency range of 1 MHz to 1 Hz at 278 to 338 K. The measurements were performed using CR2032 coin-type cells equipped with two parallel stainless-steel (SUS316L) electrodes in a thermostatically controlled container. The sample cell was thermally equilibrated in the container at 333 K at least 1 h before the measurements. Raman spectroscopy was performed using a dispersion Raman spectrometer equipped with a 532.2-nm wavelength laser at 298 K. Cyclic voltammetry (CV) measurements (SP-150, Bio-Logic) were conducted using CR2032 coin-type cells with Ni as the working electrode and Li foil as the counter electrode at a scan rate of 1 mV s⁻¹.

High-energy X-ray total scattering (HEXTS) measurements were conducted at ambient temperature using an X-ray diffraction apparatus (BL04B2 beamline at Spring-8, JASRI, Japan).³ Monochromatized 61.4 keV X-rays were obtained using a Si(220) monochromator. The observed X-ray scattering intensities were corrected for absorption, polarization, and incoherent scattering

to determine coherent scattering intensities, $I_{\text{coh}}(q)$.⁴⁻⁶ The experimental X-ray structure factor, $S^{\text{exp}}(q)$, per stoichiometric volume was expressed as follows:

$$S^{\text{exp}}(q) = \frac{\frac{I_{\text{coh}}(q)}{N} - \sum n_i f_i(q)^2}{\{\sum n_i f_i(q)\}^2} + 1$$

where n_i and $f_i(q)$ correspond to the number and atomic scattering factor of atom i , respectively, and N is the total number of atoms in the stoichiometric volume. The radial distribution function, $G^{\text{exp}}(r)$ was obtained by the inverse Fourier transform of $S^{\text{exp}}(q)$:

$$G^{\text{exp}}(r) - 1 = \frac{1}{2\pi^2 r \rho_0} \int_0^{q_{\text{max}}} q \{S^{\text{exp}}(q) - 1\} \sin(qr) W(q) dq$$

where ρ_0 corresponds to the number density of atoms, q_{max} corresponds to the maximum value of q (25 \AA^{-1} in this study) and $W(q)$ corresponds to Lorch window function.

$$W(q) = \frac{\sin(\pi q/q_{\text{max}})}{\pi q/q_{\text{max}}}$$

The MD simulations were performed with the GROMACS 2018.8 program under the NTP ensemble condition controlled by the Nose-Hoover thermostat^{7, 8} (at 298 K and 1 atm). To ensure the random starting configuration, firstly, we mixed Li^+ , TFSA^- , and PEG ($M_w = 600$) molecules at high temperature and pressure (1000 K and 1000 atm, respectively) for 1 ns. The composition (i.e., the number of LiTFSA ion pair and PEG in a cubic cell is listed in Table S1. The resulting box size at the equilibrium state are also listed in Table S1. The total simulation time was set as 15.0 ns for all the systems examined. The X-ray weighted structure factors $S^{\text{MD}}(q)$ and radial distribution functions $G^{\text{MD}}(r)$ were obtained by analyzing the data collected at 0.1 ps intervals during the last 500 ps. CLaP and OPLS-AA force fields, including intermolecular Lennard-Jones (LJ) and coulombic interactions and intramolecular interactions with (1) bond stretching, (2) angle bending, and (3) torsion of dihedral angles, were used for TFSA and PEG (see Table S2).⁹⁻¹¹ The LJ parameter for Li ions (see the Li salt/carbonate solvent system¹²) was used. The LJ parameters and partial charges used in this work are listed in Table S2. The $S^{\text{MD}}(q)$ functions were calculated using the trajectory from the MD simulations as follows:

$$S^{\text{MD}}(q) = \begin{cases} \frac{\sum_i \sum_j \left\{ \frac{n_i(n_j - 1)f_i(q)f_j(q)}{N(N-1)} \right\}}{\left\{ \sum_k \left(\frac{n_k f_k(q)}{N} \right)^2 \right\}} \int_0^{r'} 4\pi r^2 \rho_0 \left\{ g_{ij}^{\text{MD}}(r) - 1 \right\} \frac{\sin qr}{qr} dr + 1 & (i = j) \\ \frac{\sum_i \sum_j \left\{ \frac{2n_i n_j f_i(q)f_j(q)}{N^2} \right\}}{\left\{ \sum_k \left(\frac{n_k f_k(q)}{N} \right)^2 \right\}} \int_0^{r'} 4\pi r^2 \rho_0 \left\{ g_{ij}^{\text{MD}}(r) - 1 \right\} \frac{\sin qr}{qr} dr + 1 & (i \neq j) \end{cases}$$

where n_i and N are the number of i atoms and the total number of atoms in the simulation box, and $g_{ij}^{\text{MD}}(r)$ is the atom-atom pair correlation function between atoms i and j . The $G^{\text{MD}}(r)$ was obtained from the calculated $S^{\text{MD}}(q)$, conducting a similar procedure to that of HEXTS.

Determination of μ values.

The density of the cross-linking points (μ) was estimated by using polymer concentration (c) and p values, which was based on the tree-like theory.¹³ According to the tree-like models, the relationship between c and p is described as follows. $P(F_A^{\text{out}})$ is the probability that a chain does not yield to an infinite network; $P(F_A^{\text{out}}) = (1/p - 3/4)^{1/2} - 1/2$. $P(X_n)$ is the probability that tetra-arms become n -arm cross-linking points. Thus, $P(X_3)$ and $P(X_4)$ can be estimated using the following equations; $P(X_3) = {}_4C_3 P(F_A^{\text{out}})[1 - P(F_A^{\text{out}})]^3$ and $P(X_4) = {}_4C_4 [1 - P(F_A^{\text{out}})]^4$. Consequently, the density of the cross-linking points (μ) is given by the following equation: $\mu = c(P(X_3) + P(X_4))$, where c values are the concentration of tetra-arm polymer (TetraPEG). In this work, we used the experimental p values determined from (1) k_{gel} ' value and (2) second-order rate equation (i.e., 95 wt% for all TetraPEG electrolytes with Li/O_{PEG} = 1:10, 1:4, and 1:1). The μ values were thus calculated to be 4.3×10^{-2} , 2.7×10^{-2} , and $9.6 \times 10^{-3} \text{ cm}^3 \text{ mol}^{-1}$ for Li/O_{PEG} = 1:10, 1:4, and 1:1 systems, respectively.

Table S1. The composition (i.e., the number of polymer, cation, and anion) and box length of the systems in the simulation box.

Type	linear PEG (M_w : 600)	Li ⁺	TFSA ⁻	Box length / Å
Li/O _{PEG} = 1:10	172	223	223	58.88
Li/O _{PEG} = 1:4	135	439	439	60.64
Li/O _{PEG} = 1:1	66	860	860	64.04

Table S2. Force field parameters for PEG,^{10,11} TFSA⁻,⁹ and Li⁺¹² used in the MD simulation.

	labeling	σ (Å)	ϵ (kcal mol ⁻¹)	q (e)
PEG	H _P	2.50	0.030	0.03
	C _P	3.50	0.066	0.14
	C _O	3.50	0.066	0.11
	C _E	3.50	0.066	-0.18
	O _P	2.90	0.140	-0.40
TFSA ⁻	F	2.95	0.053	-0.16
	C	3.50	0.066	0.35
	O	2.96	0.210	-0.53
	S	3.55	0.250	1.02
	N	3.25	0.170	-0.66
Li ⁺	Li	1.46	0.191	1.00

Bond	K_r (kcal mol ⁻¹ Å ⁻²)	r_{eq} (Å)
H _P – C _P	340.0	1.090
C _P – O _P	320.0	1.410
C _P – C _P	310.0	1.526
C _O – H _P	340.0	1.090
C _O – O _P	320.0	1.410
C _P – C _E	310.0	1.526
C _E – H _P	340.0	1.090
F – C	883.6	1.323
C – S	470.8	1.818
S – O	1274.1	1.442

S – N	744.0	1.570
Angle	K_θ (kcal mol ⁻¹ rad ⁻²)	θ_{eq} (deg)
H _P – C _P – H _P	35.0	109.5
C _P – C _P – O _P	50.0	109.5
C _P – O _P – C _P	60.0	109.5
H _P – C _P – C _P	50.0	109.5
H _P – C _P – O _P	50.0	109.5
H _P – C _O – H _P	35.0	109.5
H _P – C _O – O _P	50.0	109.5
C _O – O _P – C _P	60.0	109.5
H _P – C _E – H _P	35.0	109.5
C _P – C _E – H _P	50.0	109.5
O _P – C _P – C _E	50.0	109.5
H _P – C _P – C _E	50.0	109.5
F – C – F	186.7	107.1
F – C – S	165.9	111.8
C – S – O	207.9	102.6
C – S – N	195.0	100.2
O – S – N	188.6	113.6
S – N – S	160.4	125.6
O – S – O	231.6	118.5

Torsion	V ₁ (kcal mol ⁻¹)	V ₂ (kcal mol ⁻¹)	V ₃ (kcal mol ⁻¹)
H _P – C _P – C _P – H _P	0.000	0.000	0.318
O _P – C _P – C _P – H _P	0.000	0.000	0.468
C _P – C _P – O _P – C _P	0.650	-0.250	0.670
H _P – C _P – O _P – C _P	0.000	0.000	0.760
H _P – C _E – C _P – H _P	0.000	0.000	0.318
O _P – C _P – C _E – H _P	0.000	0.000	0.468
C _P – O _P – C _P – C _E	0.650	-0.250	0.670
H _P – C _O – O _P – C _P	0.000	0.000	0.760
C _O – O _P – C _P – C _P	0.650	-0.250	0.670

$O_P - C_P - C_P - O_P$	1.740	-0.157	0.279
$C_O - O_P - C_P - H_P$	0.000	0.000	0.760
$F - C - S - O$	0.000	0.000	0.347
$F - C - S - N$	0.000	0.000	0.316
$C - S - N - S$	7.833	-2.490	-0.764
$O - S - N - S$	0.000	0.000	-0.004

PEG

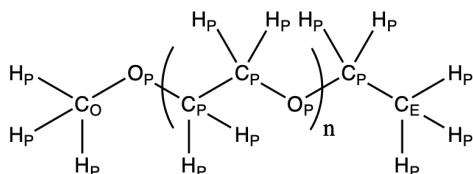
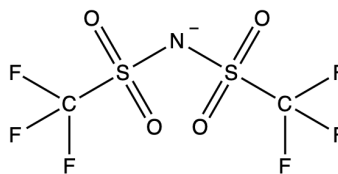
TFSA⁻

Table S3. The fitting parameters based on the VTF equation for TetraPEG solid electrolytes with $Li/TFSA/O_{PEG} = 1:10, 1:4$ and $1:1$.

Type	$\sigma_0 / mS\ cm^{-1}$	B / K	T_0 / K
$Li/O_{PEG} = 1:10$	161	641	215
$Li/O_{PEG} = 1:4$	177	806	214
$Li/O_{PEG} = 1:1$	150	1050	206

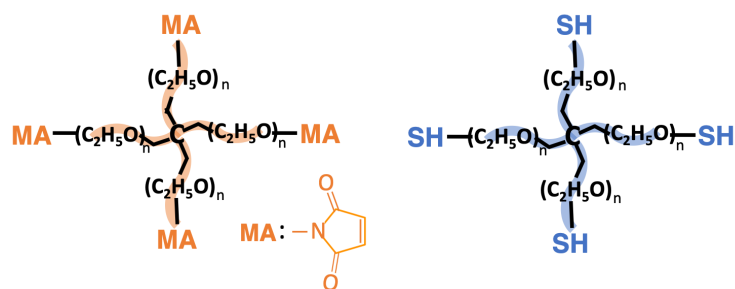


Figure S1. Chemical structures of TetraPEG-MA and TetraPEG-SH.

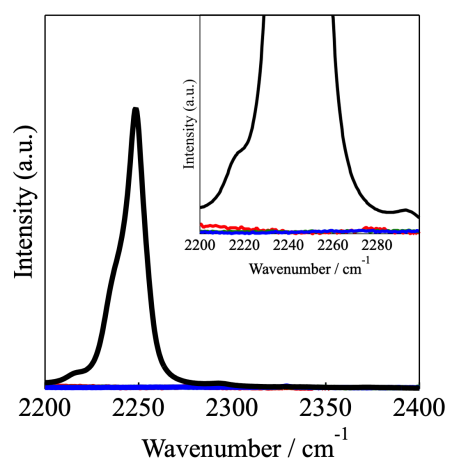


Figure S2. Raman spectra observed for the TetraPEG electrolytes with Li/O_{PEG} = 1:10 (green), 1:4 (blue), and 1:1 (red), together with that for neat BN (black).

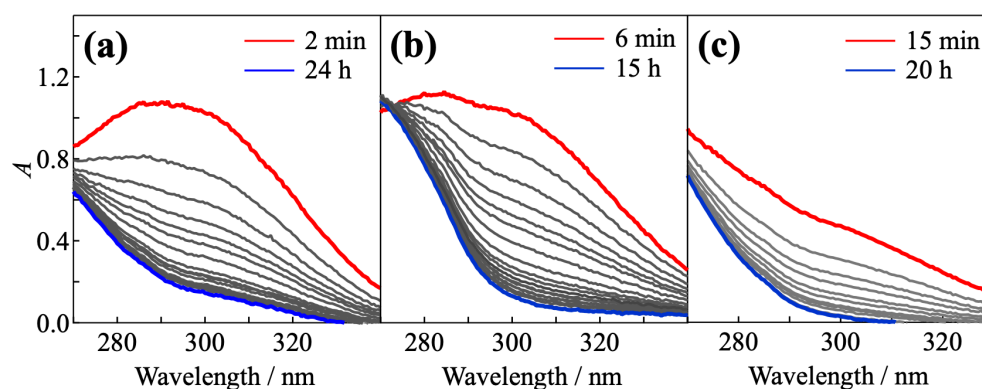


Figure S3. Time-dependent UV-vis spectra for the TetraPEG gelation in LiTFSA/BN solutions with Li/O_{PEG} = (a) 1:1, (b) 1:4, and (c) 1:10. The total polymer content in the solution was fixed at 10 wt% for all systems.

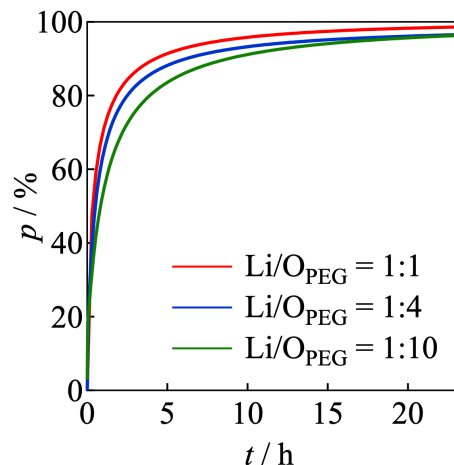


Figure S4. The reaction efficiency (p) calculated using the k_{gel}' values for the TetraPEG gelation in LiTFSA/BN solutions with $\text{Li}/\text{O}_{\text{PEG}} = 1:10$ (green), $1:4$ (blue), and $1:1$ (red).

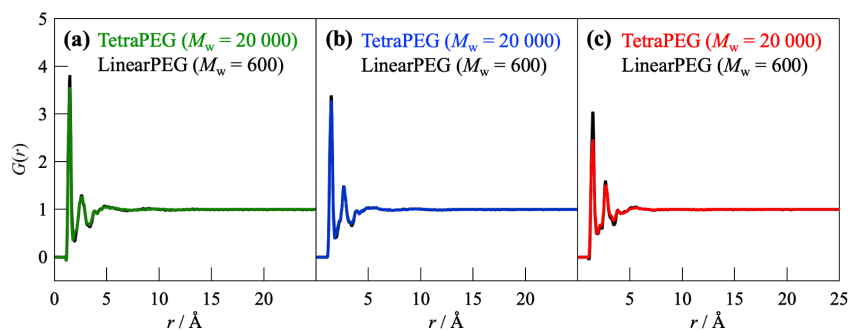


Figure S5. $G^{\text{exp}}(r)$ profiles obtained from HEXTS measurements for the TetraPEG electrolytes with $\text{Li}/\text{O}_{\text{PEG}} =$ (a) $1:10$, (b) $1:4$, and (c) $1:1$, together with those for the LiTFSA/PEG electrolytes using linear PEG ($M_w = 600$).

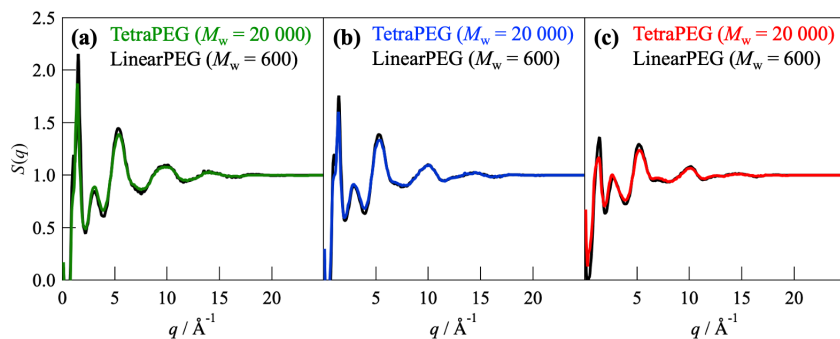


Figure S6. $S^{\text{exp}}(q)$ profiles obtained from HEXTS measurements for the TetraPEG electrolytes with $\text{Li}/\text{O}_{\text{PEG}} =$ (a) $1:10$, (b) $1:4$, and (c) $1:1$, together with those for the LiTFSA/PEG electrolytes using linear PEG ($M_w = 600$).

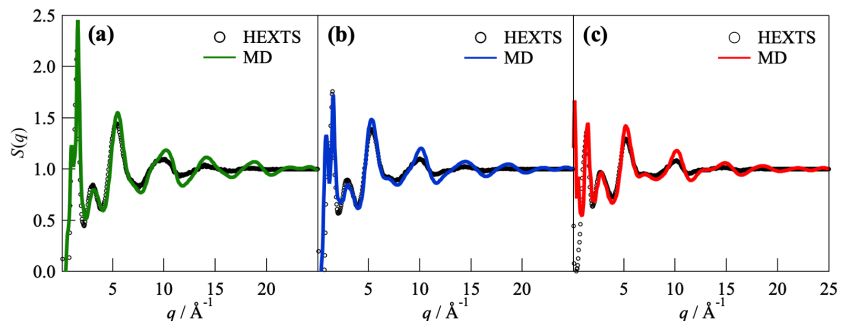


Figure S7. $S^{\text{exp}}(q)$ and $S^{\text{MD}}(q)$ profiles obtained from HEXTS measurements (open circles) and MD simulations (solid lines) for the LiTFSA/PEG electrolytes using linear PEG with $\text{Li}/\text{O}_{\text{PEG}} =$ (a) 1:10, (b) 1:4, and (c) 1:1.

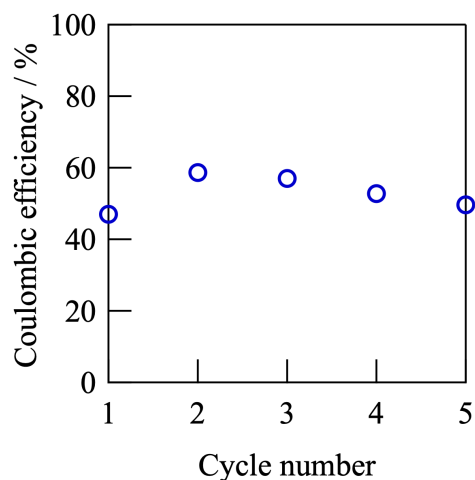


Figure S8. Coulombic efficiencies of the TetraPEG electrolyte with $\text{Li}/\text{O}_{\text{PEG}} = 1:4$. The efficiency values were calculated using the integrated reductive and oxidative currents in the CV profile.

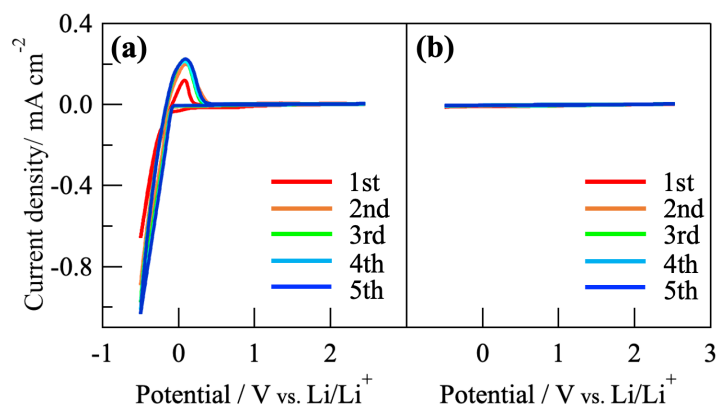


Figure S9. Cyclic voltammograms for the Ni electrode in the TetraPEG electrolytes with $\text{Li}/\text{O}_{\text{PEG}} =$ (a) 1:10 and (b) 1:1 at 333 K; scan rate: 1.0 mV s^{-1} .

References

1. A. Ishikawa, T. Sakai and K. Fujii, *Polymer*, 2019, **166**, 38-43.
2. A. Ishikawa, N. Ikeda, S. Maeda and K. Fujii, *Phys. Chem. Chem. Phys.*, 2021, **23**, 16966-16972.
3. S. Kohara, K. Suzuya, Y. Kashihara, N. Matsumoto, N. Umesaki and I. Sakai, *Nucl. Instrum. Meth. A*, 2001, **467-468**, 1030-1033.
4. S. Sakai, *KEK Report 90-16*, National Laboratory for High Energy Physics, Tsukuba, Japan, 1990.
5. D. T. Cromer, *J. Chem. Phys.*, 1969, **50**, 4857-4859.
6. J. H. Hubbell, W. J. Veigele, E. A. Briggs, R. T. Brown, D. T. Cromer and R. J. Howerton, *J. Phys. Chem. Ref. Data*, 1975, **4**, 471.
7. S. Nosé, *Mol. Phys.*, 1984, **52**, 255-268.
8. W. G. Hoover, *Physical review A*, 1985, **31**, 1695-1697.
9. J. N. C. Lopes and A. A. H. Pádua, *J. Phys. Chem. B*, 2004, **108**, 16893-16898.
10. W. D. Cornell, P. Cieplak, C. I. Bayly, I. R. Gould, J. Kenneth M. Merz, D. M. Ferguson, D. C. Spellmeyer, T. Fox, J. W. Caldwell and P. A. Kollman, *J. Am. Chem. Soc.*, 1995, **117**, 5179-5197.
11. W. L. Jorgensen, D. S. Maxwell and J. Tirado-Rives, *J. Am. Chem. Soc.*, 1996, **118**, 11225-11236.
12. J.-C. Soetens, C. Millot and B. Maigret, *J. Phys. Chem. A*, 1998, **102**, 1055-1061.
13. Y. Akagi, T. Katashima, Y. Katsumoto, K. Fujii, T. Matsunaga, U.-i. Chung, M. Shibayama and T. Sakai, *Macromolecules*, 2011, **44**, 5817-5821.